IEEE Access
Multidisciplinary ⋮ Rapid Review ⋮ Open Access Journal

Received August 7, 2021, accepted September 9, 2021, date of publication September 16, 2021, date of current version October 8, 2021.

Digital Object Identifier 10.1109/ACCESS.2021.3113299

Adaptive Model Predictive Control for DC-DC Power Converters With Parameters' Uncertainties

MOHAMED E. ALBIRA, (Student Member, IEEE), AND MOHAMED A. ZOHDY, (Senior Member, IEEE)
Department of Electrical and Computer Engineering, Oakland University, Rochester, MI 48309, USA
Corresponding author: Mohamed E. Albira (mohamedalbira@oakland.edu)

ABSTRACT This research investigates the Adaptive Model Predictive Controller (AMPC) and Linear Parameter-Varying (LPV) control system for a direct current (dc-dc) buck-boost converter, considering the parameters' uncertainty. The LPV model and the AMPC are explicitly constructed to perform a robust control design for the proposed dc-dc converter. The LPV model was created out of a set of linearized systems at different operating conditions to perform Linear Time-Invariant (LTI) models. Due to the dc-dc converter's nonlinear characteristic, the performed LTI models might have declination, which the AMPC can perfectly address by adapting the prediction model for the changes in the operating conditions. The proposed AMPC control system was implemented in a simulation environment as well as in a real-time environment on an Arduino Mega 2560 microcontroller to test its robustness and quality. The proposed AMPC control system works well compared with some existing control system algorithms at different prediction horizons. Also, the comparison considers the designed Gain Scheduling Proportional Integral (G.S-PI) and the regular Model Predictive (reg-MPC) Controllers were implemented without using the LPV model to test their performance against the proposed converter's parameters uncertainties.

INDEX TERMS DC-DC buck-boost converter, MPC controller, AMPC controller, LPV model, uncertainty modeling, quadratic programming (QP), optimization.

I. INTRODUCTION

In the real-time implementation of the dc-dc converters, there are several inconstant variables that affect their performance. The switching behavior, unsustainable power supply, and uncertainty of the parameters are all vital variables that can strongly degrade the dc-dc converter's work performance. Usually, not all of these variations are counted at the control system design. The variables mentioned can cause the system to be nonlinear. To address the degradations of these systems, many control systems approaches have been widely studied. Some researchers applied linear control approaches to govern these types of converters; however, they might fail to perform well under the various disturbances that might affect them [2]–[5]. Other studies have used the nonlinear control systems for different types of dc-dc converters [7]–[9].

Although the existing control systems have given acceptable outputs and results, they have not addressed several challenges that deeply affect the performances of the proposed dc-dc power converters. This includes faster responses, handling constraints that can govern the input and outputs of the proposed plant system, robustness against the disturbances and the variations to both the input power supply and the output load, and the interior circuit parameters' uncertainty. For instance, in note [1], a new Adaptive MPC (AMPC) was proposed for a class of constrained discrete-time linear systems with parametric uncertainties. This approach was implemented based on the min-max optimization process, using the adaptive strategy to approximate the parameters' uncertainty, and estimating the output error. The optimization feasibility and the close loop system stability are theoretically approved. A global robust tracking controller for the dc-dc buck converter uses multiple techniques to take the uncertainty of the capacitance and the inductance into consideration. The nonlinear emulation method is used to consider all the benefits of the nonlinear feedback design technique, in addition to the domination technique. Also, the discrete time reduced order observer was used to estimate the unmeasurable system states [2]. In study [6], an online adaptive controller was studied to ensure that the output was tracking the reference signal in the presence of large values of parametric, non-parametric,

The associate editor coordinating the review of this manuscript and approving it for publication was Mohsin Jamil.

matched, and mismatched perturbations at the buck converters' working time. The authors in [10] investigated the Robust Model Predictive Controller (RMPC), which replaced the inner system model with a set of LTI models. This was called an uncertain plant model, where the min-max out of these models were used to minimize the worst-case values over this set. However, this approach is complex for online implementations. The paper [11] introduced a new methodology to characterize the system's uncertainties for the Robust Model Predictive Controller (RMPC). This approach approximately found the system's uncertainties by the convex hull computing algorithm. This method uses a sampling approach to find a finite set of the generated systems. After that, the convex hull finds the most significant set that represent the closed plant and the robust optimization is performed by evaluating the constraints only to the extreme points. In [22] A novel re-formulation of MPC as a sparse non-condensed Quadratic Programming (QP) problem is implemented based on a set of LPV models. Due to the LPV models' changes over time, the model equations' equality constraints are not removed to get a condensed quadratic programming problem. The optimization will take a longer time to calculate the QP problem at every sampling time. Therefore, the system was reformulated as a piecewise-affine-equations given by the Karush-Kuhn-Tucker conditions of optimality and solved using the Newton-method and exact line search quickly. In [30] An offset free finite set control-MPC controller (OFFCS-MPC) and higher order sliding mode observer (HOSO) has been implemented for dc-dc buck converter feeding constant power loads (CPL) with unknown load variations and parameter's uncertainties. Although the OFFCS-MPC performed very robust controlling the dc-dc buck converter, the resultant high computational burden makes it requires higher speed, and bigger memory in terms of hardware; it is also not suitable to work for bilinear converters such as boost or buck-boost dc-dc power converters.

In this paper, the AMPC control scheme was implemented to control a dc-dc buck-boost converter which was:

- Linearized at different operating conditions to perform a set of LTI models; those models define a Linear Parameter-Varying (LPV) model.
- Designed assuming that the uncertainty parameters were not precisely known but they were bounded in a min-max range.
- Applied constraints to limit the amplitude of the input control signal within a boundary of 0 and highest value of the duty cycle d.
- Its performance tested at different prediction horizons.

The AMPC control system for the proposed converter was implemented in real time using Arduino Mega 2560 microcontroller and it works well to provide the desired output voltage at different levels and in fast response.

The paper is structured as follows: in section II, the design of the dc-dc buck-boost converter is presented. Section III represents the AMPC controller design strategy and algorithm. In Section IV, a Simulating and Experiment results comparisons are presented. Finally, the discussion and conclusion of the proposed work are evaluated in Sections V.

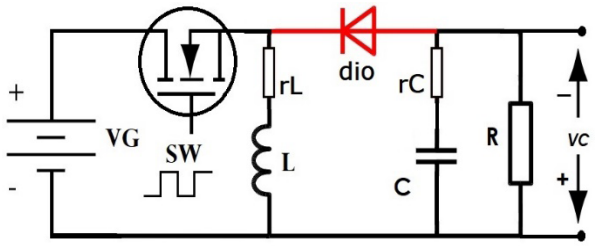

FIGURE 1. DC-DC buck-boost converter schematic circuit.

II. DC-DC BUCK-BOOST DYNAMIC SYSTEM DESIGN

The first step toward accurate system design is to carefully consider most of the details that represent the real-time system. Mathematical modeling is the way to approximate the physical system dynamics [12]. The precise system outputs and results come when the differences, or the error between the mathematical modeling and the real physical system, are minimized.

Applying the Kirchhoff's voltage and current laws to the dc-dc buck-boost schematic circuit in Fig. 1 to illustrate the inductor current iL and output voltage vC. It should be noted that this paper considers the proposed converter which works in a continuous condition mode (CCM), where the parameters' values and the operation modes in the CCM have been deeply studied and guaranteed in [13] and [17]. The parameters in the circuit diagram are the VG for the input voltage, the SW represents the switching behavior of the MOSFET, L for the inductor, **dio** for the diode, C for the capacitor, rC and $\mathcal{C}$ for the capacitor and inductor resistors, R for the resistive load, Ts is the sampling time, and d for the duty cycle [16].

Due to the switching behaviors SW ON and OFF, two working modes can therefore be generated (the ON mode and OFF mode). By multiplying those two modes with the duty cycle d and $(1-\mathrm{d})$ respectively, and adding them together, the averaged model can be illustrated [14]. For simplicity, the dynamics of the switching behaviors will be ignored in this paper and the reader is referred to [13], [17] for more details.

A. THE LINEARIZATION PROCESS

The averaged model of the dc-dc buck-boost converter leads to the differential equations that is used to illustrate the averaged inductor current iL(t) and the capacitor voltage vC (t) .

$$\frac{\mathrm{diL}\,(\mathrm{t})}{\mathrm{dt}} = \left(-\frac{-\mathrm{rL}\,(\mathrm{R}+\mathrm{rC})-(\mathrm{R}*\mathrm{rC})\,(1-\mathrm{d})}{\mathrm{L}\,(\mathrm{R}+\mathrm{rC})}\right)\mathrm{iL}\,(\mathrm{t}) - \left(\frac{\mathrm{R}\,(1-\mathrm{d})}{\mathrm{L}\,(\mathrm{R}+\mathrm{rC})}\right)\mathrm{vC}\,(\mathrm{t}) + \left(\frac{-\mathrm{d}}{\mathrm{L}}\right)\mathrm{vG}\,(\mathrm{t}) \quad (1)$$

$$\frac{\mathrm{dvC}\,(\mathrm{t})}{\mathrm{dt}} = \left(\frac{\mathrm{R}\,(1-\mathrm{d})}{\mathrm{C}\,(\mathrm{R}+\mathrm{rC})}\right)\mathrm{iL}\,(\mathrm{t}) - \left(\frac{1}{\mathrm{C}\,(\mathrm{R}+\mathrm{rC})}\right)\mathrm{vC}\,(\mathrm{t}) \quad (2)$$

Obviously, from equations (1) and (2), the system is nonlinear due to the multiplication terms of the time-varying quantities of the inductor current iL (t) , capacitor voltage vC (t), and the input voltage vG (t) with the duty cycle d. Therefore, for the aim of linear control design, this nonlinear behavior must be linearized around equilibrium points. After a given number of sampling periods, the converter reaches the steady state conditions. This means that the duty cycle d = D and the input voltage vG(t) = VG reach the constant values, applying the inductor-volt second balance and the capacitor charge balance principles and the small-ripple approximations, to illustrate the steady state or (DC values) of the inductor current and the capacitor voltage values.

$$\mathrm{IL} = -\frac{\mathrm{VC}}{(1-\mathrm{D})\mathrm{R}},\ \mathrm{VC} = -\frac{\mathrm{D}}{(1-\mathrm{D})}\mathrm{VG},\ \mathrm{D} = \frac{\mathrm{VC}}{\mathrm{VC}+\mathrm{VG}} \tag{3}$$

Since the expressions in (3) are at the steady state conditions (constant DC values), their derivatives will be zero. To derive the small-signal ac model that perturbs around the steady state operating points of the IL and VC, the input voltage vG(t) and the duty cycle d will be assumed to be equal to the values at the steady state operating points of the given VG, D and the perturbations as they represented with a hat on them ($\widetilde{.}$) [17] and [18].

$$\begin{aligned} \mathrm{vG}(t) &= \mathrm{VG} + \widetilde{\mathrm{vG}}(t),\ \mathrm{d}(t) = \mathrm{D} + \widetilde{\mathrm{d}},\ \mathrm{iL}(t) \\ &= \mathrm{IL} + \widetilde{\mathrm{iL}}\mathrm{vC}(t) = \mathrm{VC} + \widetilde{\mathrm{vC}}, \end{aligned} \tag{4}$$

Note that the ac small perturbations ($\widetilde{.}$) are much smaller than the steady-state values considered in the averaged model in equations (1) and (2). The linearized system is performed by separating the ac small signals from the steady-states variables. Then, the linearized dynamic model can be represented as a continuous-time state-space system as in the expression below:

$$\begin{aligned} \dot{\tilde{\mathrm{x}}} &= \mathrm{A_s}\tilde{\mathrm{x}}(t) + \mathrm{B_s}\tilde{\mathrm{u}}(t) \\ \mathrm{y} &= \mathrm{C_s}\tilde{\mathrm{x}}(t) \end{aligned} \tag{5}$$

$$\mathrm{A_s} = \begin{pmatrix} -\dfrac{(-\mathrm{rL})(\mathrm{R}+\mathrm{rC}) - (\mathrm{R} * \mathrm{rC}))\mathrm{D}'}{\mathrm{L}(\mathrm{R}+\mathrm{rC})} & -\dfrac{\mathrm{RD}'}{\mathrm{L}(\mathrm{R}+\mathrm{rC})} \\ \dfrac{\mathrm{RD}'}{\mathrm{C}(\mathrm{R}+\mathrm{rC})} & \dfrac{-1}{\mathrm{C}(\mathrm{R}+\mathrm{rC})} \end{pmatrix},$$

$$\mathrm{B_s} = \begin{pmatrix} \dfrac{\mathrm{VG}}{\mathrm{L}} \\ 0 \end{pmatrix}$$

$$\mathrm{C_s} = \begin{pmatrix} 0 & 1 \end{pmatrix},\ \mathrm{D_s} = 0 \tag{6}$$

where the $\mathrm{A_s}, \mathrm{B_s}, \mathrm{C_s}$ and $\mathrm{D_s}$ are the system state, input, output state and output noise matrices. The system state $\tilde{\mathrm{x}} = \left[\widetilde{\mathrm{iL}}\widetilde{\mathrm{vC}}\right]^{\mathrm{T}}$ represents the inductor current and the capacitor voltage. The system input $\tilde{\mathrm{u}} = \tilde{\mathrm{d}}$ are the ac small signal duty cycle (the control input signal), the y = VC is the system output, the term $\mathrm{D}' = 1 - \mathrm{D}$, and the epression $(.)^{\mathrm{T}}$ signifies the transpose of a vector or a matrix [13], [15]–[18].

B. LINEAR PARAMETER-VARYING (LPV) MODELING

The behaviors of the parameter's uncertainties generate a set of models (family of models). Over time, this set of the models creates what is called a Linear Parameter-Varying (LPV). The LPV is a linear system that has been stated depending on time-varying parameters called scheduling parameters p (t) . The scheduling parameters can be represented as a scalar quantity or a vector of different variables to define an LPV model. The LPV is modeled in a state space format that uses the coefficients which are parameter dependent [19]. In this work, the parameters' values of the proposed dc-dc converter are not precisely known; they are assumed to vary within min/max boundaries. For that issue, the linearization process was conducted over a grid of operating points. Each operating space is a subset parametrized by the scheduling parameters' values at a specific time. Over time, these subsets became a family of linear time-invariant (LTI) arrays; this configures the LPV model.

In this paper, the proposed dc-dc buck-boost converter's parameters are bounded in the representation as in the expression below:

$$\mathrm{R} \in \left[\overline{\mathrm{R}}, \underline{\mathrm{R}}\right],\ \mathrm{Vg} \in \left[\overline{\mathrm{VG}}, \underline{\mathrm{VG}}\right],\ \mathrm{L} \in \left[\overline{\mathrm{L}}, \underline{\mathrm{L}}\right] \quad \text{and } \mathrm{C} \in \left[\overline{\mathrm{C}}, \underline{\mathrm{C}}\right] \tag{7}$$

The change in the scheduling parameters' values directly affects the LPV scheduled state-space matrices $\mathrm{S_p} = (\mathbf{A_p}(\mathrm{p}), \mathbf{B_p}(\mathrm{p}), \mathbf{C_p})$, the matrix $\mathbf{C_p}$ is assumed known as in (9). The nominal values for the plant inputs, states, and output are specified to go with its scheduled state-space matrices parallelly. This method helps the AMPC controller to configure the correct LTI model and the corresponding operating points over a considered prediction horizon to project the system output. To the aim for a discrete-time control design, the set linearized LTI models are discretized using the Zero Order Hold (ZOH) method at a sampling time Ts. Therefore, the discrete LPV system can be expressed as below:

$$\begin{aligned} \tilde{\mathrm{x}}(\mathrm{k}+1) &= \mathbf{A_p}(\mathrm{p})(\tilde{\mathrm{x}}(\mathrm{k})) + \mathbf{B_p}(\mathrm{p})(\tilde{\mathrm{u}}(\mathrm{k})) \\ \tilde{\mathrm{y}}(\mathrm{k}) &= \mathbf{C_p}(\mathrm{p})(\tilde{\mathrm{x}}(\mathrm{k})) \end{aligned} \tag{8}$$

where k (k > 0) is the discrete time period, $\tilde{\mathrm{x}}(\mathrm{k}) \in \mathbb{R}^{2\times 1}$ is the system states vector, $\tilde{\mathrm{u}}(\mathrm{k}) \in \mathbb{R}^{1\times 1}$ is the control input (manipulated variable (MV)), $\tilde{\mathrm{y}}(\mathrm{k}) \in \mathbb{R}^{1\times 1}$ is the system measured outputs (MO). The $\mathbf{A_p}(\mathrm{p}) \in \mathbb{R}^{2\times 2}\mathbf{B_p}(\mathrm{p}) \in \mathbb{R}^{2\times 1}$ and $\mathbf{C_p} \in \mathbb{R}^{1\times 2}$ are the discrete time LPV scheduled state-space matrices depending on the scheduling parameters (p).

Due to the rank of the pair matrices ($\mathbf{A_p}$, and $\mathbf{B_p}$) and the matrices ($\mathbf{A_p}$, and $\mathbf{C_p}$) the system is controllable and observable.

And the LPV scheduling matrices are represented:

$$\mathbf{A_p} = \begin{pmatrix} -\dfrac{(-rL)(R+rC)-(R*rC))D'}{L(R+rC)} & -\dfrac{RD'}{L(R+rC)} \\ \dfrac{RD'}{C(R+rC)} & \dfrac{-1}{C(R+rC)} \end{pmatrix}$$
$$\mathbf{B_p} = \begin{pmatrix} \dfrac{VG}{L} \\ 0 \end{pmatrix}$$
$$\mathbf{C_p} = \begin{pmatrix} 0 & 1 \end{pmatrix} \tag{9}$$

III. CONTROL SYSTEM DESIGN

As previously mentioned, the LPV model is comprised of LTI models that are linearized at various operating conditions, which can approximately describe the proposed converter working range. Therefore, the AMPC control system is the proposed control method to resolve these changes in the proposed plant model. To this end, the AMPC controller designed offline at the initial operating conditions using the system matrices $(\mathbf{A_p}(0),\mathbf{B_p}(0),\mathbf{C_p})$ which are considered fully known. Then, the implemented AMPC at the initials will be incremented at the run time based on the information from the LPV model and the converter feedback signals [15], [16], [19]–[21].

A. ADAPTIVE MODEL PREDICTIVE CONTROL (AMPC) DESIGN

Due to the parameters changes, the system matrices keep changing over time. The AMPC is the perfect control approach due to its capability to update the prediction model and the operating conditions. Once they are updated, they remain constant over a prediction horizon interval. The AMPC is an online optimization based using the QP optimization approach. This optimization is tuned based on the system measurements in real-time, and the scheduling parameters predictions.

Since the cost function is a quadratic and the constraints are affine. The performing of the incremented optimization formula solved every time instant, formulated as below:

$$\underbrace{\min}_{\Delta u} \sum_{m=1}^{Np-1} (\widetilde{y}(k+m\,|\,k) - y_{rf}(k+m))^T Q_x (\widetilde{y}(k+m\,|\,k) - y_{rf}(k+m)) + \sum_{m=0}^{Nc-1} \Delta\widetilde{u}(k+m)^T R_u \Delta\widetilde{u}(k+m) \tag{10a}$$

$$\begin{aligned} \text{s.t. } \widetilde{x}(k+m+1|k) &= \mathbf{A_p}(p)(\widetilde{x}(k+m|k)) + \mathbf{B_p}(p)(\widetilde{u}(k+m|k)) \\ \widetilde{y}(k+m+1|k) &= \mathbf{C_p}(p)(\widetilde{x}(k+m+1|k)) \\ \widetilde{x}(k\,|\,k) &= \widetilde{x}(k) \\ y_{rf}(k+Nr+s) &= y_{rf}(k+Nr+s-1) \\ m &= [0,\ldots,Np-1] \\ s &= [0,\ldots,Np-Nr-1] \end{aligned} \tag{10b}$$

where Np, Nc and Nr are so-called the prediction horizon, the control horizon and the span of reference window, Q_x and R_u are the tracking error, and control input rate of change weighting matrices respectively.

At the prediction time period m, The reference state vector $\widetilde{x}(k+m|k)$ is an incremental of the state vector $\widetilde{x}$ at time $k+m$, depending on pre-known information at time instant k. The input control sequence $\Delta\widetilde{u}(k+m|k)$ is an incremented vector of the previous input control sequence $\widetilde{u}(k-1)$, and the output reference vector $y_{rf}(k+m)$, can be predicted in advance at time period m. Therefore, cost minimization of the problem (10) can be done using the quadratic programming (QP) which is redefined interims of the scheduled state-space matrices S_p as below:

$$\begin{aligned} &\underbrace{\min}_{\xi} \frac{1}{2}\xi^T \mathcal{H}(p)\,\xi + \Gamma(k)^T \mathcal{W}(p)^T \xi \\ &\text{s.t. } G_\emptyset(k)\,\xi \le W_\emptyset(k)\,\Gamma(k) + \mathcal{S}_\emptyset(k) \end{aligned} \tag{11}$$

where the $\xi \in \mathbb{R}^{n_s}$ is the optimization vector. The $\Gamma(k) = \left[\widetilde{x}(k)\ y_{rf}(k)\ \widetilde{u}(k-1)\right]$ is a vector of the variable parameters that change over time, and the matrices for the QP problem (11) are illustrated as below:

$$\mathcal{H}(k) = \mathcal{M}(p(k))^T Q_x \mathcal{M}(p(k)) + R_u \tag{12a}$$
$$\mathcal{W}(k) = \mathcal{M}(p(k))^T Q_x \widetilde{\mathcal{F}}(p(k)) \tag{12b}$$

where the hessian matrix $\mathcal{H}$ and the column vector $\mathcal{W}$ are sequences of the optimal control inputs, the $\bar{I} \in \mathbb{R}^{n_u \times n_u}$, and the input and output constraints are illustrated as below [24]–[27]

$$U^{min}(k) = \begin{pmatrix} u^{min}(k) \\ \vdots \\ u^{l}(k+Nc-1) \end{pmatrix},$$
$$U^{max}(k) = \begin{pmatrix} u^{max}(k) \\ \vdots \\ u^{max}(k+Nc-1) \end{pmatrix}$$
$$Y^{man}(k) = \begin{pmatrix} y^{min}(k) \\ \vdots \\ y^{min}(k+Np-1) \end{pmatrix},$$
$$Y^{max}(k) = \begin{pmatrix} y^{max}(k) \\ \vdots \\ y^{max}(k+Np-1) \end{pmatrix} \tag{13}$$

And

$$\begin{aligned} Q_x &= \mathrm{diag}(Q_x(k),\ldots,Q_x(Np-1)) \\ R_u &= \mathrm{diag}(R_u(k),\ldots,R_u(Nc-1)) \end{aligned} \tag{14}$$

The prediction for the future reference of the scheduling parameters is computed by considering the pre-known information about the optimization vector, which is solved at $k-1$ iteration over a prediction horizon Np. Thus, the AMPC adaptive process solves the optimization problem using the predicted scheduling parameters reference which keeps the objective QP cost function and the subjected constraints

$$W_{\emptyset}(k) = \begin{pmatrix} \bar{I} & 0 & 0 & 0 \\ \bar{I} & 0 & 0 & 0 \\ \bar{I} & \mathcal{F}(k) & 0 & 0 \\ \bar{I} & -\mathcal{F}(k) & 0 & 0 \end{pmatrix}, \quad \mathcal{S}_{\emptyset}(k) = \begin{pmatrix} -U^{min}(k) \\ U^{max}(k) \\ -Y^{min}(k) \\ Y^{max}(k) \end{pmatrix}$$

$$\widetilde{\mathcal{F}_p}(k) = \mathcal{F}_p(k) \begin{pmatrix} I^{(n_y \times 1)} & 0 & \dots & 0 \\ \dots & \dots & \dots & \dots \\ 0 & \dots & 0 & I^{(n_y \times 1)} \\ 0 & \dots & 0 & I^{(n_y (Np-Nr) \times 1)} \end{pmatrix}, \quad G_{\emptyset}(k) = \begin{pmatrix} -\gamma(k) \\ \gamma(k) \\ -\mathcal{M}(k) \\ \mathcal{M}(k) \end{pmatrix} \tag{15}$$

$$\mathcal{F}_p(k) = \begin{pmatrix} \widetilde{C_p}(k)\widetilde{A_p}(k) \\ \widetilde{C_p}(k)\widetilde{A_p}^2(k) \\ \vdots \\ \widetilde{C_p}(k)\widetilde{A_p}^{Np}(k) \end{pmatrix}, \quad \gamma(k) = \begin{pmatrix} \bar{I} & 0 & 0 & \dots & 0 \\ \bar{I} & \bar{I} & 0 & \dots & 0 \\ \dots & \dots & \dots & \dots & 0 \\ \bar{I} & \bar{I} & \bar{I} & \dots & \bar{I} \end{pmatrix}$$

$$\mathcal{M}_p(k) = \begin{pmatrix} \widetilde{C_p(k)}\widetilde{B_{pu}(k)} & 0 & \dots & 0 \\ \widetilde{C_p}(k)\widetilde{A_p(k)}\widetilde{B_{pu}(k)} & \widetilde{C_p}(k)\widetilde{B_{pu}}(k) & \dots & 0 \\ \vdots & \vdots & \ddots & \vdots \\ \widetilde{C_p}(k)\widetilde{A_p}^{Np-1}(k)\widetilde{B_{pu}}(k) & \widetilde{C_p}\widetilde{A_p}^{Np-2}(k)\widetilde{B_{pu}}(k) & \dots & \widetilde{C_p}(k)\widetilde{B_{pu}}(k) \end{pmatrix} \tag{16}$$

updated every time instant k. Since the LPV was stated with the scheduling parameters directly affecting the system dynamics and the input control signal manipulated by the AMPC process, the approximate relationship between the LPV scheduled state-space matrices and the control signals can be defined in a linear state equation (17).

Therefore, iterating the discrete time LPV scheduled state space matrices $S_p = (\mathbf{A_p}, \mathbf{B_p}, \mathbf{C_p})$ used to predict the scheduling parameters reference, and keep the AMPC parameters updated every time instant k over a prediction horizon Np [24]–[27].

$$\Delta\widetilde{X}_p(k|k) = \mathcal{F}_p\widetilde{X}_p(k) + \mathcal{M}_p\Delta U(k) \tag{17}$$

where the predicted future state vector $\Delta\widetilde{X}_p(k)$, the future input control sequence $\Delta U(k)$ are the LIT vector based on the scheduling parameters S_p are incremented at the time instant k over a prediction horizon Np as below

$$\Delta\widetilde{X}_p(k) = \left[\Delta\widetilde{X}_p(k+1), \dots, \Delta\widetilde{X}_p(k+Np \mid k)\right]^T \tag{18a}$$

$$\Delta U(k) = \left[\Delta u(k \mid k), \dots, \Delta u(k+Nc-1 \mid k)\right]^T \tag{18b}$$

And the matrices $\mathcal{M}_p$ and $\mathcal{F}_p$ are computed in (16) which are defined by the scheduling parameters state matrices $\mathcal{S}_p$.

By incrementing the expression (17), the prediction of the scheduling parameters is estimated to keep the AMPC optimization of the proposed objective cost function, and the constraints (11) updated each time instant k over the considered prediction horizon Np.

To get the QP problem's (11) solved instantly over a prediction horizon interval, the scheduling parameters reference need to be defined, and the LPV scheduled state-space matrices calculated as below [24]–[27].

$$S_p(k+i) = \begin{cases} S_p(k \mid k) & \text{if } i = 0 \\ S_p(k+i|k) & \text{if } 0 < i \le Np \\ S_p(k+Np \mid k) & \text{Otherwise} \end{cases} \tag{19}$$

TABLE 1. Parameters value for the converter for simulation model.

Parameters		Nominal Value	Variations
Input voltage	VG	5 V	-/+ 20%
Inductor	L	100 uH	-10/+ 90%
Inductor resistive	rL	0.1 Ω	0%
Capacitor	C	220 uF	-10/+ 90%
Capacitor resistive	rC	0.1 Ω	0%
Resistive Load	R	1 KΩ	-/+ 20%
Switching frequency	fs	25 kHz	0%
Duty cycle	d	calculated	0%
Sampling time	Ts	0.00004 sec	0%

IV. SIMULATION AND EXPERIMENT

As projected in this paper, the proposed dc-dc buck-boost converter is designed based on the values of the parameters, which are illustrated in Table 1. The variety in the L, C, VG, and R parameters lead to create multiple system models, each model different than the others. Therefore, to cover this variety, these models implemented and linearized at the operating points associated with it, as it is computed in section II-A. Thus, the system with such multiple models can hardly be controlled using a regular control scheme. Therefore, the AMPC, reg-MPC and G.S-PI are implemented to test

Algorithm 1 The AMPC Algorithm Constructed as Below: [24] and [27]

Pre-known the input control sequence U(k|k-1), the plant state vector $\widetilde{x_p}(k)$, the estimated parameters state vector $\widetilde{X_p}(k)$, the plant output $\widetilde{y}(k)$, the implemented set of the LPV model, the prediction matrices $\mathcal{M}_p$, $\mathcal{F}_p$

1) $U(k\,|\,k-1) \rightarrow u(k-1)$;
2) $\left(x_p(k), y_{rf}(k), u(k-1)\right) \rightarrow \Gamma(k)$;
3) $\widetilde{X_p}(k|k-1) = \mathcal{F}_p(k)\,\widetilde{X_p}(k) + \mathcal{M}_p(k)\,\Delta U(k|k-1)$;
4) **for** m = m:Np − 1
5) **if** m = 0 then $S_p(k) = S_p(p(k))$;
6) Else if m ≤ Np − 1 then $S_p(k) = (p(k+m|k-1))$;
7) Else $S_p(k) = S_p(p(k+Np-1\,|\,k-1))$;
8) **End if**; **End if**; **End for**;
9) $\mathcal{H}(k) = \mathcal{M}(k)^T Q_x(k)\mathcal{M}(k) + R_u(k)$
10) $\mathcal{W}(k) = \mathcal{M}(k)^T Q_x(k)\mathcal{F}(k)$
11) $G_\emptyset(k) = G_\emptyset\left(S_p(p(k)), \ldots, S_p(p(k+Np))\right)$
12) $W_\emptyset(k) = W_\emptyset\left(S_p(p(k)), \ldots, S_p(p(k+Np))\right)$
13)

$$z^*: \underbrace{\min}_{\xi} \tfrac{1}{2}\xi^T\mathcal{H}(p)\,\xi + \Gamma(k)^T\mathcal{W}(p)^T\xi$$

$$\text{s.t.} \quad G_\emptyset(k)\,\xi \le W_\emptyset(k)\,\Gamma(k) + \mathcal{S}_\emptyset(k)$$

14) $\xi^* \rightarrow \Delta U(k)$
15) $U(k) = U(k-1) + \Delta U(k)$;

Output: Only the first element of the predicted control signal U(k) applied to the system

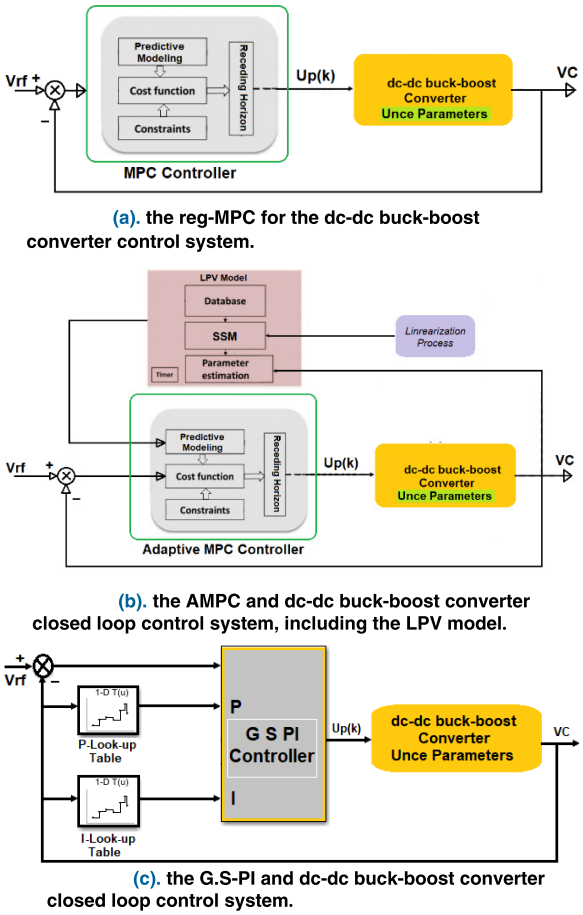

FIGURE 2. (a) The reg-MPC for the dc-dc buck-boost converter control system. (b) The AMPC and dc-dc buck-boost converter closed loop control system, including the LPV model. (c) The G.S-PI and dc-dc buck-boost converter closed loop control system.

their performances against such a system with parameters' uncertainties.

Figure. 2a and b illustrate the closed loop system for the dc-dc buck-boost converter, which is a single-input and single-output (SISO) control system. The input control signal $\widetilde{u} = \widetilde{d}$ is the manipulated variable (MV) and the system output is the capacitor voltage VC which is a measured output (OU) signal. As mentioned above, the goal is to design linear control systems capable of handling the dc-dc converter with the parameters' uncertainties. The closed loop of reg-MPC is designed without the use of the LPV model and it is designed using the nominal plant model. But in the running time, the converter will be influenced by the change in the parameter's values. The AMPC controller is designed offline with a one system model at the initial condition values as we did in the reg-MPC design. Then at the running time, the AMPC keeps updating its prediction model and calculating the objective cost function online using the information coming from the LPV model and the converter's feedback signal to match the changes in the system parameters. Both the reg-MPC and the AMPC are proposed to handle the inequality constraints applied to the input control signal U. The prediction horizon Np is varied to test their effectiveness on the system performance and outputs. The weighting matrices Q_x and R_u are valued as follow:

$$Q_x = \text{diag}[1, \ldots, 1], \quad R_u = \text{diag}[1, \ldots, 1] \qquad (20)$$

Also, in this paper, a Gain Scheduling proportional and integral (G.S-PI) control system was considered to test its robustness and performance against the uncertainties of the parameters in the proposed dc-dc buck-boost converter. In the design of the G.S-PI controller, the lock-up tables were used to store the P and I gains that were calculated offline for every linearized model of the proposed dc-dc buck-boost converter. Figure. 2c shows the G.S-PI buck-boost converter's closed-loop control system structure using the look-up tables. The result and outputs of this control system were compared with the implemented the reg-MPC and the AMPC control systems.

The projected reg-MPC, AMPC and G.S-PI for the proposed dc-dc buck-boost converter were simulated using the MATLAB and SIMULINK environment (version R-2020B) which are carried out on a laptop computer with CORE i7 1.8GHz CPU, 16 GB RAM, and a WINDOWS 10 professional operating system. This control system scheme was designed using the MPC, the AMPC, the lock-up table, the PID, and the LPV models in Simulink Toolboxes.

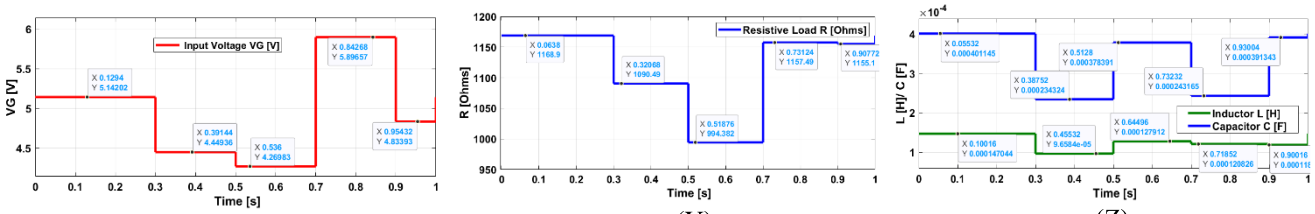

FIGURE 3. X) for the input voltage (VG), Y) for the resistive load (R) values, and Z) for the values of the inductor (L) and the capacitor (C).

A. SIMULATION ANALYSIS AND RESULTS

As it is proposed in this paper, the dc-dc buck-boost converter was implemented with parameters R, L, C and VG varied over time. Therefore, the three proposed control systems were implemented to test their performance and robustness against these variants. Figure. 3 (X, Y, and Z) show the values of the input voltage VG in a range between minimum 4.27V and maximum 5.89V, a resistive load R minimum value of 0.994 K Ohms and maximum value of 1.169 K Ohms, a inductor L ranged between 9.66e-5 H and maximum 147e-6 H, and a capacitor C valued between 234e-6 F to 401e-6 F.

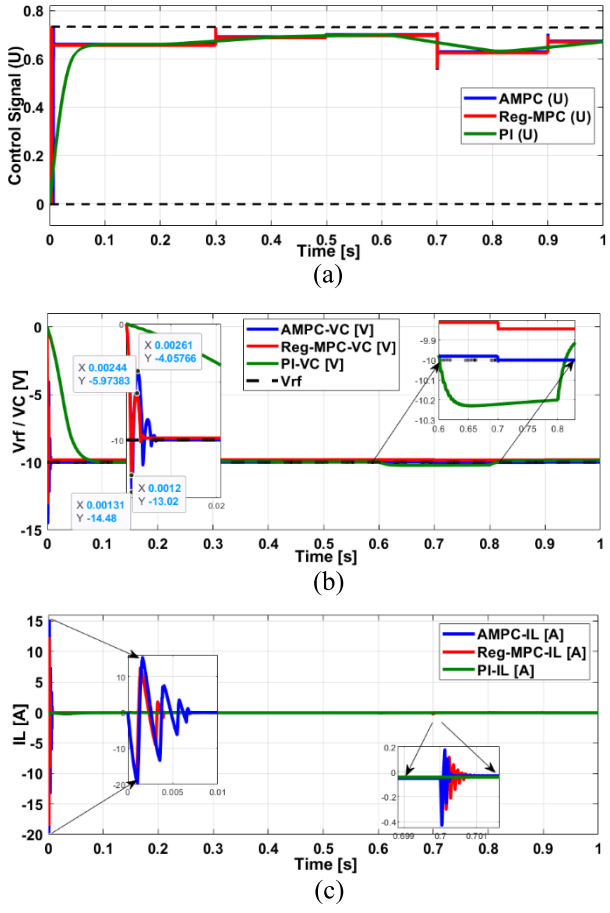

FIGURE 4. (a, b, and c) show the control signal (U), the reference voltage (Vrf), the closed loop system output voltage (VC), and the inductor current (iL) for all targeted control systems.

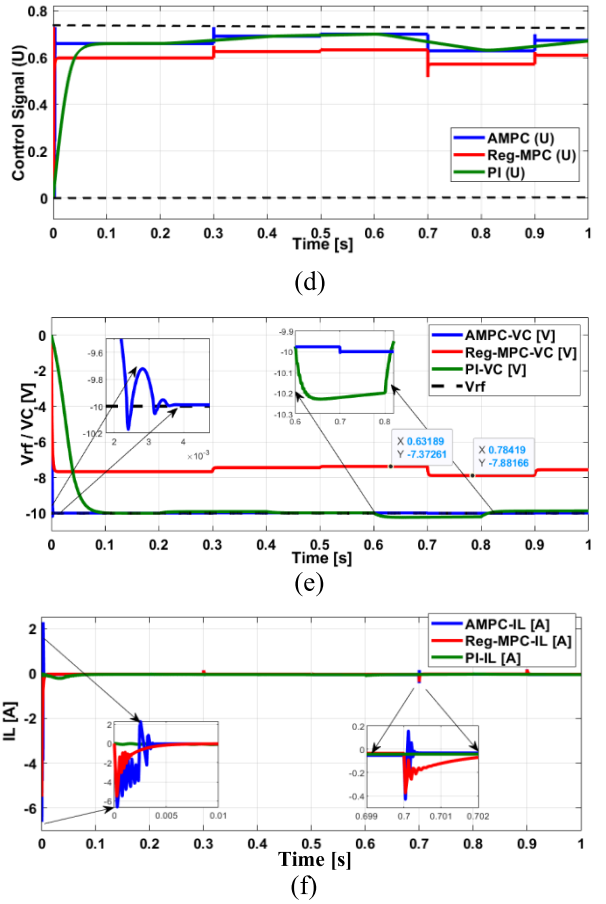

FIGURE 5. (d, e, and f) show the control signal (U), the reference voltage (Vrf), the closed loop system output voltage (VC), and the inductor current (iL) for all targeted control systems.

Figures. 4 and 5 show the performance of the reg-MPC and the AMPC when the prediction horizon was valued at Np = 10 and Np = 100 respectively, the control horizon Nc = 3, and the weighting matrices Q_x and R_u are valued as in the equation (20). The G.S-PI controller's gains listed in the TABLE.2.

Figures . 4a and 5d represent the targeted control systems' input control signal U and the applied constraints to the AMPC and the reg-MPC controllers. Figure. 4b shows the AMPC, and the reg-MPC controllers were easily guided the dc-dc converter output voltage very fast to track the reference signal (Vrf) with an overshoot percentage of 50% in

TABLE 2. Shows the calculated gains for the G.S-PI controller.

Time	0 – 0.3	0.3-0.5	0.5-0.7	0.7-0.9	0.9 – 1
Kp	-1.25e-5	-1.31e-5	-1.43e-5	-1.80e-5	-1.86e-5
Ki	-0.625	-0.653	-0.716	-0.898	-0.931

TABLE 3. Shows the output voltage VC percentage steady state error (E_{ss}), overshoot (O_S), and settling time (sT).

Time	0 to 0.3 sec			0.6 to 0.8 sec	
	E_{ss} %	O_S %	sT sec	E_{ss} %	O_S %
AMPC	0	50	0.008	0	0
reg-MPC	0	30	0.004	3	0
G.S-PI	0.5	0	0.1	2.5	0

TABLE 4. Shows the output voltage VC percentage steady state error (E_{ss}) overshoot (O_S) and settling time (sT).

Time	0 to 0.3 sec			0.6 to 0.8 sec	
	E_{ss} %	O_S %	sT sec	E_{ss} %	O_S %
AMPC	0	3	0.004	0	0
reg-MPC	25	0	0.004	27	0
G.S-PI	0.5	0	0.1	2.5	0

TABLE 5. Shows the number of iterations at different prediction horizons.

Algorithms	Np=10		Np=20		Np=30	
	Min	Max	Min	Max	Min	Max
AMPC	1	8	1	7	1	7
qpOASES	2	12	11	20	21	35
GPAD	1	17	1	26	1	37

the AMPC and 30% in the reg-MPC; however, the G.S-PI was performing butter with no overshooting but responding very slow to reach the desired output voltage level, this is in the first time period from 0 to 0.3 sec. In the time period between 0.6 sec to 0.8 sec, although the converter parameters changed with high values, all the controllers performed well with a tiny percentage of steady state error. Figure. 4c shows the inductor current iL, which is considered an unmeasured output signal. Although it starts with some oscillations at each time period, they get to the stability quickly; this is the performance of the AMPC and the reg-MPC controllers. On the other hand, no oscillations in the inductor current iL performed by the G.S-PI control system. More details listed in the TABLE.3.

The performance of the AMPC and reg-MPC changed because of the change in the control horizon value Np = 100. There was no change in the G.S-PI controller performance since the same gains were used for the same parameters' values. In Figure. 5e, despite a slight overshooting of 3%, the AMPC was able to force the output voltage VC to reach the steady-state condition at the desired value in a very fast time. Although the parameters' values in the proposed dc-dc converter are varied, the AMPC shows high flexibility to pick the suitable LTI array from the LPV model, which matches these changes in the converter's parameters each time. The same figure shows the reg-MPC performed poorly to track the reference signal Vrf. It performed with a high amount of a steady-state error about 25% in the time period between 0 sec to 0.3 sec, and its performance became worse with the change in converter parameters. Also, the performance of the G.S-PI controller is well, but in the period between 0.6 sec to 0.8, the output voltage has some steady-state error of 2.5%. More details can be found in TABLE. 4. Figure. 5f shows the inductor current, which is considered as an unmeasured output signal. Although it starts with some oscillating, they get stable quickly; this is in AMPC and reg-MPC controllers' performance, and no oscillations in the G.S-PI controller performance.

B. COMPARISION WITH OTHER EXISTING CONTROL APPROACHES

In this sub-section, the proposed AMPC control system is compared with the offset free finite set MPC (OFFS-MPC) control algorithm [30] in terms of the steady state error, the percentage overshoot, and the settling time. Despite the OFFCS-MPC shows high robustness and performances in terms of the settling time around 2 ms, the percentage of the voltage overshooting less than 1%, and smoothly tracking the reference voltage signal with 0% steady state error percentage, the impacts of the value changes in the resistive load, the inductor, the capacitor, and the input voltage when they all happen at the same time have not been shown. On the other hand, although the proposed AMPC control scheme relatively has a slower response and higher voltage overshooting, its performance remains very well although all the system parameters, including the input voltage VG and the resistive load R have a high percentage of uncertainties applied at the same time. In terms of the inductor current iL, the OFFCS-MPC system obviously has no control over it. Therefore, the iL is highly impacted by the uncertainties in the system parameters. In contrast, although the inductor current iL is counted as an unmeasured output signal in the proposed AMPC control system, the stability in the output voltage VC positively affected the inductor current iL performance.

Also, the proposed AMPC control system was compared with some existing MPC control algorithms. The comparison was in the number of the iterations at different prediction horizons Np = 10 to 30 increased by 10. The max-iteration was set to 1000, and the terminal tolerance was 0.001. the proposed AMPC control system compared with the online active set solver (qpOASES) algorithm [28], and the Accelerated Dual Gradient Projection (GPAD) algorithm [29] as detailed in the TABLE. 5.

From TABLE.5, the AMPC has the lowest numbers of the maximum iterations between 7 to 8 iterations. On the other hand, the compared control algorithms' iteration numbers increased as the prediction horizon Np was increased.

Another side of the comparison is in regards to the hardware cost, which was done with two of the MPC algorithms that exist in the literature. As mentioned above, the proposed AMPC control system was implemented in real-time using Arduino Mega 2560, which costs about $15 based on the price from the Amazon website [31]. In contrast, the algorithms in the references [22] and [30] were implemented on relatively high priced hardware systems. That concludes that the proposed AMPC optimization process does not require a heavy computation burden, which can be carried on a simple microprocessor such as the Arduino Mega 2560.

C. REAL TIME EXPERIMENT AND RESULTS

The AMPC and LPV control system for the dc-dc buck-boost converter was implemented and built on an Arduino Mega microcontroller, which is an ATmega 2560 CPU, with 54 digital input/output, 16 analog inputs. Also, it is provided with 256 bytes flash memory size for the code storage and CPU clock speed of 16MHZ. The proposed real time control system was coded and implemented using the MATLAB, SIMULINK 2020B and the ARDUINO support packages. Figures. 6 and 7 show the real-time closed loop control system and the toolboxes that were used to build the connectivity between the implemented Simulink model to the Arduino Mega and the real-time dc-dc buck-boost converter circuit.

There were four signals fed to the Simulink model from the external via the Arduino analog blocks and one signal sent to the dc-dc buck-boost converter through the Arduino PWM block. These signals are the feedback voltage, feedback current, reference voltage, input voltage, and the control signal U. The feedback voltage and current signals were measured and fed back from the converter. The reference voltage Vrf was measured and fed from a separate DC voltage source, and the input voltage signal came from a DC voltage source. The control signal U sent as a PWM signal to the dc-dc buck-boost converter as they can be seen in Figures. 6 and 7.

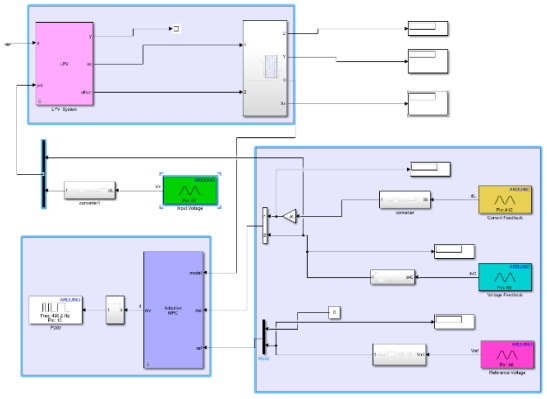

FIGURE 6. The Simulink model of the AMPC and LPV control system for the dc-dc buck-boost converter.

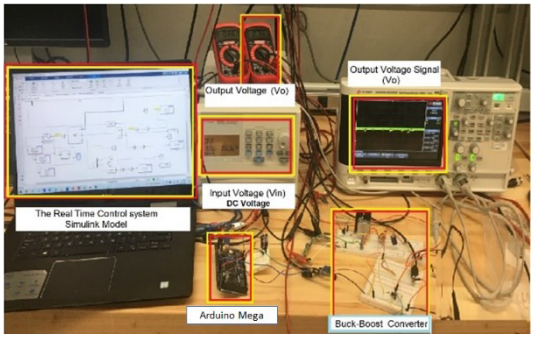

FIGURE 7. The Real time experiment for the closed loop AMPC and LPV for the dc-dc buck boost converter.

The dc-dc buck-boost circuit was built on a breadboard with components values, L = 100 uH for the inductor, the capacitor C = 1000 uF, resistive load R = 0.9 to 1.2 K Ohm, and the input voltage VG = 5 V DC. Since the Arduino cannot read the negative voltage values, an inverting operation amplifier (op-amp) was built to invert the proposed converter negative output voltage and fed to the Arduino using the ACS712 Module voltage and current sensor.

Figures.8-10 represent the output of the proposed AMPC for the dc-dc buck-boost converter closed-loop control

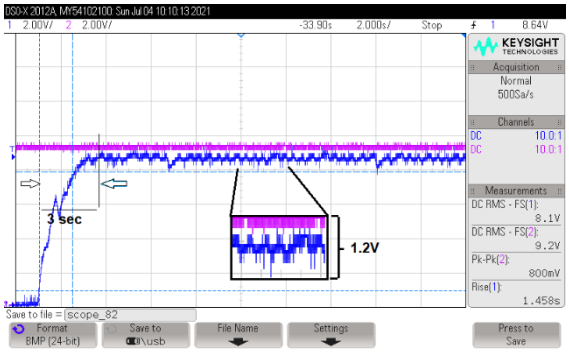

FIGURE 8. Shows the output voltage (VC = 8.1V) when the Reference voltage (Vrf = 9.2V), the Input voltage (Vin = 5V) and Resistive load R = 1k ohms.

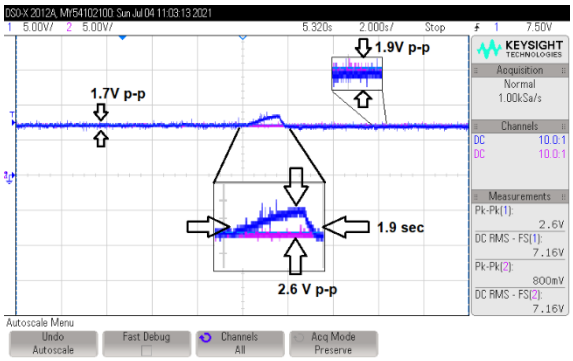

FIGURE 9. Shows the output voltage (VC = 7.16V) when the Reference voltage (Vrf = 7.16V), the Input voltage (Vin = 5V) and Resistive load R = 1k ohms to 1.2k Ohms.

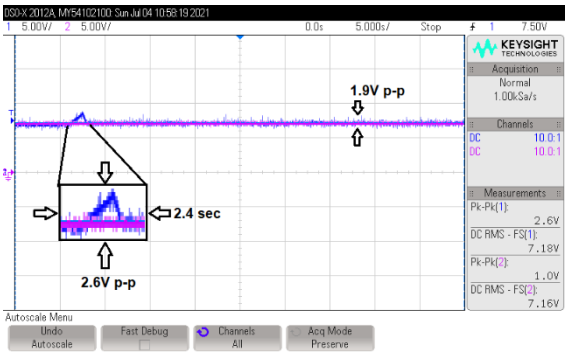

FIGURE 10. Shows the output voltage (VC = 7.18V) when the Reference voltage (Vrf = 7.16V), the Input voltage (Vin = 5V) and Resistive load R = 0.9k ohms to 1k Ohms.

system, measured by the oscilloscope over the channels numbered 1 and 2. Channel 1 (blue) is the output voltage, and channel 2 (purple) is the reference voltage signals.

As shown in Figures. 8-10, the controller works very well to track the reference signal Vrf. In Figure. 8, the input voltage VG was set to 5V DC, and the reference signal was Vrf = 9.2V. The output voltage was fast in reaching the steady-state condition in about 3 sec and the rise time RT of 1.4 sec with some steady-state errors E_{ss} of approximately 11.9%. Also, the proposed control system robustness was tested against the sudden changes in the resistive load. During the running time, the resistive load was changed from 0.9 to 1.2 K Ohms. The output was well maintained to be kept at the desired output; although the load was changed suddenly, the AMPC control system inquired about 1.9 sec to bring the output voltage signal back to the 7.16V as it can be seen in Figure. 9. The load in Figure. 10 was changed from 0.9K Ohms to 1K Ohm, and the control system was very well responded. It takes about 2.4 sec to bring the output back to the desired output voltage.

The output voltage range was limited up to 10 volts maximum that was due to the op amp range which limited to 10 DC volt; however, the system without the op amp can go up to −25V DC.

V. CONCLUSION

In this paper, the AMPC control system was implemented to control a dc-dc buck-boost converter. The proposed dc-dc converter was modeled with the parameters' uncertainty, assuming this converter was supplied from an unsustainable input voltage source VG; also, the resistive load R, the capacitor C, and the inductor L were assumed to vary over time. These variances and the dc-dc converter's original switching behaviors made it acts as a nonlinear system model. Therefore, to apply a linear AMPC control scheme to such a nonlinear system, the proposed plant model linearized at different operating conditions to create a set of LTI models covering the proposed dc-dc converter working range. A discrete LPV model was then modeled as an array of state-space models representing this converter system's varying dynamics based on the scheduling parameters. To this end, the AMPC at the beginning was designed using a linearized model at the initial plant model and the initial operating condition. The prediction modeling and online optimization are then updated based on the converter's feedback signals and data from the discrete LPV model depending on the changes in the converter's parameters. The AMPC continues updating its predicted plant model and the operating conditions over a prediction horizon to maintain constant output values tracking the applied reference signal. The performance of proposed AMPC control approach was compared in terms of the performance with some of the excepting MPC approaches [28]–[30]. Also the proposed AMPC results and outputs were compared with the results of designed reg-MPC and G.S-PI control systems, which were modeled without using the LPV model. Then the AMPC algorithm implemented in real-time using an Arduino Mega 2560 microcontroller. From the comparison, it is concluded that the proposed AMPC control algorithm highly performed in terms of the system outputs quality, its real-time optimization requires relatively low computational burden, as well as in regards to the cost, the used hardware is cheap in the price, which can be simply implemented at a simple laboratory using MATLAB and Simulink built-in functions and toolboxes, and the Simulink Arduino support packages.

REFERENCES

[1] B. Zhu, Z. Zheng, and X. Xia, "Constrained adaptive model-predictive control for a class of discrete-time linear systems with parametric uncertainties," *IEEE Trans. Autom. Control*, vol. 65, no. 5, pp. 2223–2229, May 2020, doi: 10.1109/TAC.2019.2939659.

[2] C. Zhang, J. Wang, S. Li, B. Wu, and C. Qian, "Robust control for PWM-based DC–DC buck power converters with uncertainty via sampled-data output feedback," *IEEE Trans. Power Electron.*, vol. 30, no. 1, pp. 504–515, Jan. 2015, doi: 10.1109/TPEL.2014.2299759.

[3] A. Bemporad, F. Borrelli, and M. Morari, "Min-max control of constrained uncertain discrete-time linear systems," *IEEE Trans. Autom. Control*, vol. 48, no. 9, pp. 1600–1606, Sep. 2003, doi: 10.1109/TAC.2003.816984.

[4] D. Q. Mayne, S. V. Rakovic, R. Findeisen, and F. Allgower, "Robust output feedback model predictive control for constrained linear systems under uncertainty based on feed forward and positive invariant feedback control," in *Proc. 45th IEEE Conf. Decis. Control*, San Diego, CA, USA, Dec. 2006, pp. 6618–6623, doi: 10.1109/CDC.2006.376851.

[5] Z. Qian, O. Abdel-Rahman, H. Al-Atrash, and I. Batarseh, "Modeling and control of three-port DC/DC converter interface for satellite applications," *IEEE Trans. Power Electron.*, vol. 25, no. 3, pp. 637–649, Mar. 2010, doi: 10.1109/TPEL.2009.2033926.

[6] T. K. Nizami, A. Chakravarty, and C. Mahanta, "Time bound online uncertainty estimation based adaptive control design for DC–DC buck converters with experimental validation," *IFAC J. Syst. Control*, vol. 15, Mar. 2021, Art. no. 100127.

[7] S. Hiti and D. Borojevic, "Robust nonlinear control for boost converter," in *Proc. IEEE Power Electron. Spec. Conf. (PESC)*, Seattle, WA, USA, Jun. 1993, pp. 191–196, doi: 10.1109/PESC.1993.471945.

[8] J. Alvarez-Ramirez, G. Espinosa-Perez, and D. Noriega-Pineda, "Current-mode control of DC-DC power converters: A backstepping approach," in *Proc. IEEE Int. Conf. Control Appl. (CCA)*, Mexico City, Mexico, Sep. 2001, pp. 190–195, doi: 10.1109/CCA.2001.973862.

[9] S. Tan, Y. M. Lai, and C. K. Tse, "General design issues of sliding-mode controllers in DC–DC converters," *IEEE Trans. Ind. Electron.*, vol. 55, no. 3, pp. 1160–1174, Mar. 2008, doi: 10.1109/TIE.2007.909058.

[10] P. Karamanakos, T. Geyer, and S. Manias, "Direct voltage control of DC-DC boost converters using enumeration-based model predictive control," *IEEE Trans. Power Electron.*, vol. 29, no. 2, pp. 968–978, Feb. 2014, doi: 10.1109/TPEL.2013.2256370.

[11] H. Sartipizadeh and T. L. Vincent, "Uncertainty characterization for robust MPC using an approximate convex hull method," in *Proc. Amer. Control Conf. (ACC)*, Boston, MA, USA, Jul. 2016, pp. 2699–2704, doi: 10.1109/ACC.2016.7525326.
[12] F. Asadi, S. Pongswatd, K. Eguchi, and N. L. Trung, "Modeling uncertainties in DC-DC converters with MATLAB and PLECS," *Synth. Lectures Elect. Eng.*, vol. 3, no. 2, pp. 1–292, 2018, doi: 10.2200/S00875ED1V01Y201809EEL006.
[13] M. Modabbernia, F. K. Khoshkbijari, R. Fouladi, and S. S. Nejati, "The state space average model of buck-boost switching regulator including all of the system uncertainties," *Int. J. Comput. Sci. Eng.*, vol. 5, no. 2, p. 120, 2013.
[14] L. Po, L. Ruiyu, S. Tianying, Z. Jingrui, and F. Zheng, "Composite adaptive model predictive control for DC-DC boost converters," *IET Power Electron.*, vol. 11, no. 10, pp. 1706–1717, Aug. 2018, doi: 10.1049/iet-pel.2017.0835.
[15] M. E. Albira, A. Alzahrani, and M. Zohdy, "Model predictive speed control of DC-DC buck converter driven DC-motor with various load torque values," in *Proc. IEEE Int. IoT, Electron. Mechatronics Conf. (IEMTRONICS)*, Vancouver, BC, Canada, Sep. 2020, pp. 1–6, doi: 10.1109/IEMTRONICS51293.2020.9216459.
[16] M. E. Albira, A. Alzahrani, and M. Zohdy, "Model predictive control of DC-DC buck-boost converter with various resistive load values," in *Proc. Global Congr. Electr. Eng. (GC-ElecEng)*, Valencia, Spain, Sep. 2020, pp. 124–128, doi: 10.23919/GC-ElecEng48342.2020.9285986.
[17] R. W. Erickson and D. Maksimovic, *Fundamentals of Power Electronics*. Boston, MA, USA: Kluwer, 2001, pp. 609–630. [Online]. Available: https://www.springer.com/gp/book/9781475705591#aboutBook
[18] C. Restrepo, J. Calvente, A. Cid-Pastor, A. E. Aroudi, and R. Giral, "A noninverting buck-boost DC-DC switching converter with high efficiency and wide bandwidth," *IEEE Trans. Power Electron.*, vol. 26, no. 9, pp. 2490–2503, Sep. 2011, 10.1109/TPEL.2011.2108668
[19] The MathWorks. (2021). *Adaptive MPC*. [Online]. Available: https://www.mathworks.com/help/mpc/ug/adaptive-mpc.html?s_tid=srchtitle
[20] A. Bemporad, "Model predictive control design: New trends and tools," in *Proc. 45th IEEE Conf. Decis. Control*, San Diego, CA, USA, Dec. 2006, pp. 6678–6683, doi: 10.1109/CDC.2006.377490.
[21] L. Wang, *Model Predictive Control System Design and Implementation Using MATLAB*. London, U.K.: Springer-Verlag, 2009.
[22] Z. Liu, L. Xie, A. Bemporad, and S. Lu, "Fast linear parameter varying model predictive control of buck DC-DC converters based on FPGA," *IEEE Access*, vol. 6, pp. 52434–52446, 2018, doi: 10.1109/ACCESS.2018.2869043.
[23] J. Kim, J.-H. Park, and K.-Y. Jhang, "Decoupled longitudinal and lateral vehicle control based autonomous lane change system adaptable to driving surroundings," *IEEE Access*, vol. 9, pp. 4315–4334, 2021, doi: 10.1109/ACCESS.2020.3047189.
[24] L. Cavanini, G. Ippoliti, and E. F. Camacho, "Model predictive control for a linear parameter varying model of an UAV," *J. Intell. Robotic Syst.*, vol. 101, p. 57, Mar. 2021, doi: 10.1007/s10846-021-01337-x.
[25] P. Falcone, M. Tufo, F. Borrelli, J. Asgari, and H. E. Tseng, "A linear time varying model predictive control approach to the integrated vehicle dynamics control problem in autonomous systems," in *Proc. 46th IEEE Conf. Decis. Control*, New Orleans, LA, USA, Dec. 2007, pp. 2980–2985, doi: 10.1109/CDC.2007.4434137.
[26] A. Bemporad. *Model Predictive Control Linear Time-Varying and Nonlinear MPC*. Accessed: May 2021. [Online]. Available: http://cse.lab.imtlucca.it/~bemporad/teaching/mpc/imt/2-ltv_nl_mpc.pdf
[27] F. Borrelli, A. Bemporad, and M. Morari, *Predictive Control for Linear and Hybrid Systems*. Cambridge, U.K.: Cambridge Univ. Press, 2017, doi: 10.1017/9781139061759.
[28] H. J. Ferreau, C. Kirches, A. Potschka, H. G. Bock, and M. Diehl, "qpOASES: A parametric active-set algorithm for quadratic programming," *Math. Program. Comput.*, vol. 6, no. 4, pp. 327–363, 2014.
[29] P. Patrinos and A. Bemporad, "An accelerated dual gradient-projection algorithm for embedded linear model predictive control," *IEEE Trans. Autom. Control*, vol. 59, no. 1, pp. 18–33, Jan. 2014.
[30] Q. Xu, Y. Yan, C. Zhang, T. Dragicevic, and F. Blaabjerg, "An offset-free composite model predictive control strategy for DC/DC buck converter feeding constant power loads," *IEEE Trans. Power Electron.*, vol. 35, no. 5, pp. 5331–5342, May 2020, doi: 10.1109/TPEL.2019.2941714.
[31] Amazon.com. (2021). *SunFounder Mega 2560 R3 ATmega2560-16AU Board Compatible With Arduino*. [Online]. Available: https://www.amazon.com/SunFounder-ATmega2560-16AU-Board-Compatible-Arduino/dp/B00D9NA4CY/ref=asc_df_B00D9NA4CY/?tag=hyprod-20&linkCode=df0&hvadid=309773039951&hvpos=&hvnetw=g&hvrand=4955456828333502132&hvpone=&hvptwo=&hvqmt=&hvdev=c&hvdvcmdl=&hvlocint=&hvlocphy=9016965&hvtargid=pla-599566677804&th=1

MOHAMED E. ALBIRA (Student Member, IEEE) received the H.D. degree in electrical and electronics engineering technology from the College of Technical and Science, Misurata, Libya, in 2002, and the M.S. degree in electrical and computer engineering from Lawrence Technological University, Southfield, MI, USA, in 2015. He is currently pursuing the Ph.D. degree in electrical and computer engineering with Oakland University, Rochester, MI, USA, since 2017. His research interests include predictive control systems and power electronics.

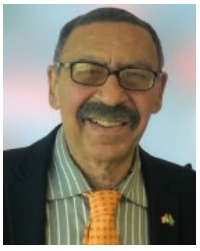

MOHAMED A. ZOHDY (Senior Member, IEEE) received the B.Sc. degree in electrical engineering from Cairo University, Egypt, in 1968, and the M.Sc. and Ph.D. degrees in electrical engineering from the University of Waterloo, Canada, in 1974 and 1977, respectively. He is currently a Professor with the School of Engineering and Computer Science, Oakland University, MI, USA. His research interests include control systems and soft computing.